Opto-Electronics Review

Dual-band absorption of a GaAs thin-film solar cell using a bilayer nano-antenna structure

A. A. M. Khalaf [a], M. D Gaballa [b]*

[a] Dept. of Electronics & Communications Engineering, Faculty of Engineering, Minia University, Minia 61111, Egypt
[b] Department of Electronics & Communications Engineering, Higher Technological Institute, 10th of Ramadan City, Egypt

Article info	Abstract
	The paper presents a dual-band plasmonic solar cell. The proposed unit structure gathers two layers, each layer consists of a silver nanoparticle deposited on a GaAs substrate and covered with an ITO layer, It reveals two discrete absorption bands in the infra-red part of the solar spectrum. Nanoparticle structures have been used for light-trapping to increase the absorption of plasmonic solar cells. By proper engineering of these structures, resonance frequencies and absorption coefficients can be controlled as it will be elucidated. The simulation results are achieved using CST Microwave Studio through the finite element method. The results indicate that this proposed dual-band plasmonic solar cell exhibits an absorption bandwidth, defined as the full width at half maximum, reaches 71 nm. Moreover, It can be noticed that by controlling the nanoparticle height above the GaAs substrate, the absorption peak can be increased to reach 0.77.

1. Introduction

Exhaustion of fossil fuels makes our community facing a lot of energy issues. It produces a lot of environmental problems and cannot meet the energy need. Sun is a plentiful energy source so the transformation of sunlight to electricity can reduce the energy crisis [1]. To make the solar cells more spreading, its cost needs to be reduced [2]. Advantages of plasmonic solar cells with a slim absorber layer are low production expenses and mechanically elastic. Disadvantage of the slim absorber layer is a poor absorption of the infrared part of the solar spectrum [3]. Nano-antenna structures have been used for light-trapping to raise the absorption of a plasmonic solar cell and, therefore, they allow the thickness of the absorber layer and the costs of the solar cell to decrease [1]. By appropriate engineering of the nanostructures, light can be condensed and bent into a slim absorber layer causing energy absorption raising [2]. There are three techniques using metallic nanostructures for light trapping in the absorber layers. First, immersed metallic nanostructures can be employed as nanoantennas due to their near-field strong effect. Second, metallic nanostructures can be employed as scattering components leading to increases in the optical path extent. Third, metallic nanostructures of the bottom surface can convert sunlight into a surface plasmonic polariton (SPP) form [1,2]. The localized surface plasmon resonance (LSPR) phenomenon of metal nanostructures leads to their extensive usage in thin-film solar cells, sensing, terahertz application, metamaterials, etc [4]. Most recently, studies have shown that nanostructures raise the light absorption in solar cells over a wide spectral range. In Ref. 4, a silicon solar cell with enhanced light absorption and raised detection sensitivity has been designed using a diamond nanoantenna array. As presented in Ref. 5, metal nanoparticles can give an efficient mechanism for expanding the photon absorption below the semiconductor bandgap in the infrared range. An effective method to increase the absorption coefficients and controlling the resonance frequency has been demonstrated in Ref. 6. A gear nanoantenna for raising the absorption of amorphous silicon solar cells has been proposed in Ref. 7. In Ref. 8, a thin-film solar cell with a wideband enhanced absorption has been designed using a periodic array of metal strips. In Ref. 3, the nanoantenna has been used to turn a vertically propagating illumination to a guiding form

*Corresponding author: minadawoud@yahoo.com

traveling into the lateral direction of the solar cell leading to enhanced absorption. In Ref. 9, an amorphous silicon solar cell with enhanced energy conversion efficiency has been designed using gold nanoparticles. A cuboid nanoparticle array for enhancing the absorption of a silicon layer in thin-film solar cells has been presented in Ref. 10. The nanoparticles can raise light absorption in the absorber layer due to their localized surface plasmon resonance [11]. Embedded nanoparticles for raising the absorption of various semiconductor materials have been presented in Ref. 12. The embedded nanoparticle can raise light absorption in the semiconductor materials due to the intensive near field zone surrounding it [5]. As illustrated in Ref. 13, light-trapping structures can give a more efficient performance compared with traditional anti-reflecting coatings. As presented in Refs. 14 and 15, embedded dielectric nanoparticle structures can give an efficient technique for enhancing the absorption in a thin-film solar cell. In Ref. 16, a thin-film solar cell with enhanced absorption has been designed using embedded lossless silica nanoparticles. A quasiperiodic photonic crystal structure for enhancing the absorption of the thin-film silicon solar cells has been proposed in Ref. 17. As shown in the results, quasiperiodic photonic crystal structures can give a more fixed performance throughout the day, as well as over the year compared with that of a periodic photonic crystal. As presented in Ref. 18, plasmonic nanoparticle arrays can provide an effective method for improving the absorption of a perovskite solar cell in the infrared range of the solar spectrum. It is found that the perovskite layer supports the absorption in visible and ultraviolet parts of the solar spectrum, while it suffers from the poor absorption of the infrared band. As demonstrated in Ref. 19, the nanoimprinted pattern on the rear contact in thin-film solar cells can give a more improved efficiency compared with that of a flat back contact. The absorption enhancements of the absorber layer using metal nanoparticles have been studied by many types of research in Refs. 20, 21 and 22. In Ref. 23, the metasurface has been used to improve the photo-generated current by means of the resonant effects. A dual-band metamaterial perfect absorber has been presented in Refs. 24. In Ref. 25, a multi-layered graphene silica-based has been used to achieve the perfect absorption over the infrared wavelength region. In Ref. 26, a broadband perfect absorber with polarization-independent has been designed to cover the spectrum from the visible to the near-infrared regime. In Ref. 27, a dual-band perfect absorber with polarization-independent has been designed to operate in the mid-infrared range. A terahertz bifunctional absorber has been presented in Ref. 28.

The solar cell can be fabricated by depositing silver nanoparticles on the absorber layer surface, then the nanoparticles are coated with anti-reflecting coatings. Fabrication of nanoparticles has been presented in Refs. 29-32. Synthesize and deposit nanoparticles on the substrate are presented in Ref. 33.

The paper presents a dual-band plasmonic solar cell. It is composed of silver nanoparticles precipitated on GaAs substrates and coated with ITO layers. In this structure, in addition to a dual-band absorption, resonance frequencies and absorption coefficients are also controlled. The geometry effect of silver nanoparticles on the resonance frequencies and absorption coefficients has been presented. A numerical investigation of the light absorption response of a proposed plasmonic solar cell by the finite element method (FEM) has been presented.

2. Structure and Design

A schematic diagram of the structure is illustrated in Fig. 1. The structure is composed of two layers, each layer from top to bottom: a silver nano-particle coated with a conductive indium tin oxide (ITO) coat, and a gallium arsenide (GaAs) substrate. Each nanoparticle consists of a cylindrical silver nanoparticle of the thickness $h = 10$ nm and an elliptical cross-section with the semi-major axis, R_L, equalling one and three tenths of the semi-minor axis, $R_s = 11$ nm. The size of the unit-cell is of 80×80 nm^2. Dielectric functions of ITO and GaAs are presumed equal to 4.67 and 12.86, respectively. The thickness of each layer is of 50 nm.
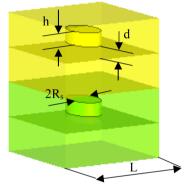

Fig.1. Structure of the proposed unit-cell. The structure is composed of two layers, the first (yellow) and the second (green).

Dispersive properties of nanoparticles are specified by the Drude model. The complex dielectric function of silver nanoparticles *vs.* the frequency can be calculated as in Eqs. (1) and (2) [34]:

$$\varepsilon_1 = \left[1 - \frac{\omega_p^2}{\omega^2 + \gamma^2} \right] \quad (1)$$

$$\varepsilon_2 = \left[\frac{\omega_p^2 \gamma}{\omega^3 + \omega \gamma^2} \right], \quad (2)$$

where ε_1 is the real portion of the complex dielectric function, ε_2 is the imaginary portion. ω_p is the electron plasma angular frequency, and γ is the angular collision frequency within the nanoparticle material [35,36].

The variance of dielectric function as a function of the wavelength λ for silver nanoparticles is illustrated in Fig. 2. For the whole of the analysis, a y-polarized plane wave is applied as an incident wave. The simulation results are achieved by the FEM method. As the proposed structure is periodic, thus the simulation domain is formed by a single unit of the structure with periodicity boundary conditions along the x-y plane. Tetrahedron mesh is used. The absorption A can be calculated as in Eq. (3) [7]:

$$A = 1 - T - R, \quad (3)$$

where $T = |S_{21}|^2$, is the transmittance and $R = |S_{11}|^2$, is the reflectance.
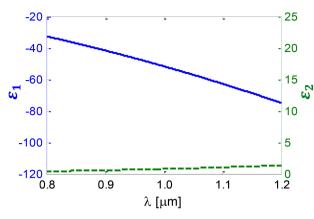
Fig. 2. The real (ε_1) and imaginary (ε_2) portions of the silver dielectric function.

3. Results and Discussion

The idea for bilayer thin-film solar cells is to basically stack two layers on top of each other. Each layer would have a different band gap, so as if part of the solar spectrum was not absorbed by the first layer, then the second would be able to absorb an additional part of the passing spectrum as shown in Figs. 3 and 4. The summation of the two absorbed parts forms two discrete absorption bands in the infra-red part of the solar spectrum as shown in Fig. 5. These layers can be optimized in order to produce a reasonable amount of power by controlling the resonance frequencies and absorption coefficients.
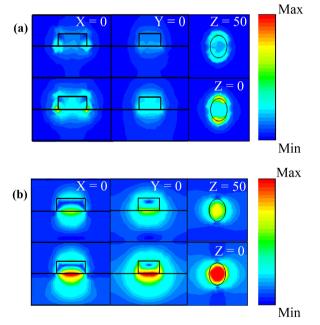

Fig. 3. Electric (a) and magnetic (b) fields distribution at high-frequency absorption peak.

The absorption response of the proposed dual-band plasmonic solar cell is presented in Fig. 5. The silver nanoparticle unit-cell is illuminated by incident light polarized along the semi-major axis R_L. As illustrated in Fig. 5, it is clear that the proposed plasmonic solar cell appears as two separate absorption peaks existing around at 0.92 μm (λ_1) and 0.98 μm (λ_2), each with absorptions of around 62%. The absorption bandwidths, known as the full width at half maximum, are of 35 nm and 29 nm at λ_1
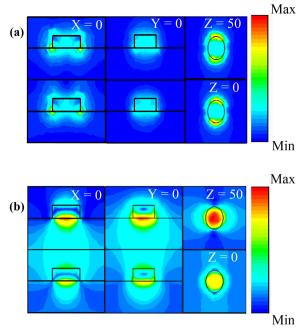

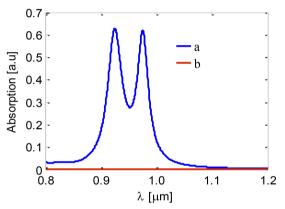Fig. 4. Electric (a) and magnetic (b) fields distribution at low-frequency absorption peak.

Fig. 5. Absorption response of the proposed solar cell with (a) and without (b) nanoparticles.

and λ_2, respectively. As shown in Fig. 5, the proposed dual-band plasmonic solar cell structure can give a more efficient performance when compared to the structure without nanoparticles.

Influence of the silver nanoparticle semi-minor axis and the thickness on the absorption coefficients and resonance frequencies is shown in Fig. 6. The silver nanoparticle unit-cell is illuminated by incident light polarized along the semi-major axis R_L. Figure 6(a) presents the influence of varying the semi-minor axis, R_s, from 11 nm to 15.5 nm, for the nanoparticle settled dimensions of: $h = 10$ nm, $L = 80$ nm, and $d = 0$. It is obvious that the proposed plasmonic solar cell structure shows two discrete absorption peaks. Both absorption peaks decrease with an increase of R_s. The high-frequency absorption peak for $R_s = 11$ nm was found at $\lambda = 0.92$ μm with the maximum absorptivity of 0.63 compared to 0.44 at $\lambda = 0.98$ μm for $R_s = 15.5$ nm. The low-frequency absorption peak for $R_s = 11$ nm was found at $\lambda = 0.98$ μm with the maximum absorptivity of 0.62 compared to 0.46 at $\lambda = 1.11$ μm for $R_s = 15.5$ nm. The frequency of both absorption peaks shifts to lower frequencies with an increase of the semi-minor axis, R_s. The FWHM increases with an increase of R_s, which is referred to a wide
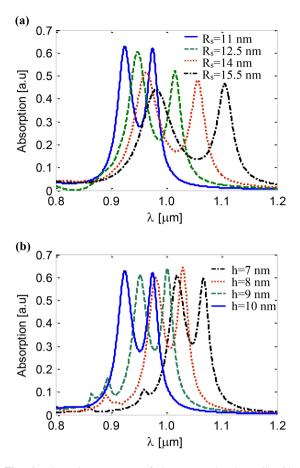
(a)

(b)

Fig. 6. Absorption response of the proposed solar cell with different nanoparticle (a) semi-minor axis and (b) thickness.

absorption range of the solar spectrum. The FWHM of the high-frequency absorption peak is of 35 nm for $R_s = 11$ nm compared to 71 nm for $R_s = 15.5$ nm while the FWHM of the low-frequency absorption peak is of 29 nm for $R_s = 11$ nm compared to 37 nm for $R_s = 15.5$ nm.

Figure 6(b) shows the absorption response of the silver nanoparticle with the various thickness, h. Other nanoparticle parameters are $R_s = 11$ nm, $L = 80$ nm, and $d = 0$. It can be observed that the proposed plasmonic solar cell has two discrete absorption peaks for all different values of the nanoparticle thickness. It can be also noticed that both absorption peaks are approximately the same. The frequency of both absorption peaks shifts to higher frequencies with an increase of the nanoparticle thickness, h. The FWHM decreases with the increase of h. The FWHM of the high-frequency absorption peak is of 45 nm for $h = 7$ nm compared to 35 nm for $h = 10$ nm while the FWHM of the low-frequency absorption peak is slightly decreased from 33 nm for $h = 7$ nm compared to 29 nm for $h = 10$ nm.

The effect of the silver nanoparticle height and periodicity on the resonance frequencies and absorption coefficients is exhibited in Figs. 7 and 8, respectively. Figure 7 reveals a reliance of the absorption response on the change of the nanoparticle height above the GaAs substrate from d = 0 to 1.25 nm. Other nanoparticle parameters are $R_s = 11$ nm, $h = 10$ nm, $L = 80$nm. As shown in Fig. 7, when the height d increases from 0 to 1.25 nm, the low-frequency absorption peak decreases and the high-frequency absorption peak increases. The high-
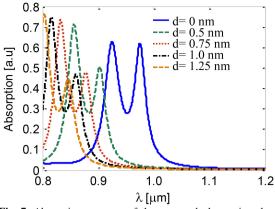

Fig. 7. Absorption response of the proposed plasmonic solar cell with different nanoparticle height.

frequency absorption peak for $d = 0$ nm was found at $\lambda = 0.92$ μm with the maximum absorptivity of 0.63 compared to 0.77 at $\lambda = 0.803$ μm for $d = 1.25$ nm. The low-frequency absorption peak for $d = 0$ nm was found at $\lambda = 0.98$ μm with the maximum absorptivity of 0.62 compared to 0.45 at $\lambda = 0.85$ μm for $d = 1.25$ nm. The FWHM of the high-frequency absorption peak is 35 nm for $d = 0$ nm compared to 30 nm for $d = 1.25$ nm. It can be noticed that when the height d increases, the FWHM of the high-frequency absorption peak slightly decreases. Both absorption peaks move toward higher frequencies as the height d increases. As shown in the results, by controlling the nanoparticle height above the GaAs substrate, the absorption peak can be increased to reach 0.77 which achieves a high current density. At these high frequencies, the photons have higher energies.

Figure 8 discusses a reliance of the absorption response on the several periods L when it varies from 60 nm to 80 nm. Other nanoparticle parameters are $h = 10$ nm, $R_s = 11$ nm, and $d = 0$. It can be seen that two absorption peaks were found. It can be noticed that when the period L increases from 60 to 80 nm, both absorption peaks increase. The high-frequency absorption peak for $L = 60$ nm was found at $\lambda = 0.92$ μm with the maximum absorptivity of 0.54 compared to 0.63 at $\lambda = 0.92$ μm for $L = 80$ nm The low-frequency absorption peak for $L = 60$ nm was found at $\lambda = 1$ μm with the maximum absorptivity of 0.53 compared to 0.62 at $\lambda = 0.98$ μm for $L = 80$ nm. The FWHM of the high-frequency absorption
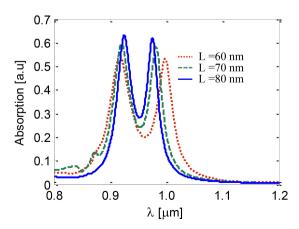

Fig. 8. Absorption response of the solar cell with nanoparticle periodicity.

peak is 49 nm for $L = 60$ nm compared to 35 nm for $L = 80$ nm while the FWHM of the low-frequency absorption peak is 36 nm for $L = 60$ nm compared to 29 nm for $L = 80$ nm. It can be seen that when the period L increases, the FWHM of both absorption peaks decreases. As illustrated in Fig. 8, when the period L increases, the low-frequency absorption peak slightly shifts to higher frequencies and the high-frequency absorption peak slightly shifts to lower frequencies.

4. Conclusions

In conclusion, a dual-band plasmonic solar cell formed by two layers of silver nanoparticle deposited on GaAs substrate and covered with ITO layer is presented. It is found that the proposed structure shows distinctive dual absorption bands. The resonance frequencies and absorption coefficients can be controlled through varying the geometry of the silver nanoparticle. As shown in the results, the proposed dual-band plasmonic solar cell achieves a full width at half maximum, reaches 71 nm. It can be noticed that by controlling the nanoparticle height above the GaAs substrate, the absorption peak can be increased to reach 0.77. The proposed structure has potential applications in the absorption of the infra-red part of the solar spectrum.

References

[1] Fei Guo, C., Sun, T., Cao, F., Liu, Q. & Ren, Z. Metallic nanostructures for light trapping in energy-harvesting devices. *Light-Sci. Appl.* **3** (4), e161 (2014).

[2] Atwater, H. A. & Polman, A. Plasmonics for improved photovoltaic devices. *Nat. Mater.* **9** (3), 205–213 (2010).

[3] Taghian, F., Ahmadi, V. & Yousefi, L. Enhanced thin solar cells using optical nano-antenna induced hybrid plasmonic travelling-wave. *J. Lightwave Technol.* **34** (4), 1267–1273 (2016).

[4] Yuan, Y.-Y. *et al.* Absorption enhancement and sensing properties of Ag diamond nanoantenna arrays. *Chinese Phys. B* **24**, 74206 (2015).

[5] Novitsky, A. *et al.* Photon absorption and photocurrent in solar cells below semiconductor bandgap due to electron photoemission from plasmonic nanoantennas. *Prog. Photovoltaics Res. Appl.* **22**, 422–426 (2014).

[6] Aboul-Dahab, M., Dawoud, M., Zainud-Deen, S.H. & Malhat, H.A. Tapered Metal Nanoantenna Structures for Absorption Enhancement in GaAs Thin-Film Solar Cells in *The 2nd International Conference on Advanced Technology and Applied Science* (ICaTAS 2017), 139–145, (2017).

[7] Medhat, M., El-Batawy, Y. M., Abdelmageed, A. K. & Soliman, E. A. Gear nano antenna for plasmonie photovoltaic. in *2016 IEEE Middle East Conference on Antennas and Propagation (MECAP)* 1–4 (2016). doi:10.1109/MECAP.2016.7790111.

[8] Pala, R. A., White, J., Barnard, E., Liu, J. & Brongersma, M. L. Design of Plasmonic Thin-Film Solar Cells with Broadband Absorption Enhancements. *Adv. Mater.* **21**, 3504–3509 (2009).

[9] Derkacs, D., Lim, S. H., Matheu, P., Mar, W. & Yu, E. T. Improved performance of amorphous silicon solar cells via scattering from surface plasmon polaritons in nearby metallic nanoparticles. *Appl. Phys. Lett.* **89**, 93103 (2006).

[10] Yuan, Z., Li, X. & Jing H. Absorption enhancement of thin-film solar cell with rectangular Ag Nanoparticles. *J. Appl. Sci.* **14** (8), 823–827 (2014).

[11] Petryayeva, E. & Krull, U. J. Localized surface plasmon resonance: Nanostructures, bioassays and biosensing—A review. *Anal. Chim. Acta* **706**, 8–24 (2011).

[12] Spinelli, P. & Polman, A. Prospects of near-field plasmonic absorption enhancement in semiconductor materials using embedded Ag nanoparticles. *Opt. Express* **20** (105), A641–A654 (2012).

[13] Simovski, C. *et al.* Enhanced efficiency of light-trapping nanoantenna arrays for thin-film solar cells. *Opt. Express* **21** (104), A714–A725 (2013).

[14] Nagel, J. R. & Scarpulla, M. A. Enhanced absorption in optically thin solar cells by scattering from embedded dielectric nanoparticles. *Opt. Express* **18** (102), A139–A146 (2010).

[15] Nagel, J. R. & Scarpulla, M. A. Enhanced light absorption in thin film solar cells with embedded dielectric nanoparticles: induced texture dominates Mie scattering. *Appl. Phys. Lett.* **102** (15), 151111 (2013).

[16] Li, B., Lin, J., Lu, J., Su, X. & Li, J. Light absorption enhancement in thin-film solar cells by embedded lossless silica nanoparticles. *J. Opt.* **15** (5), 05500 (2013).

[17] Bauer, C., & Giessen, H. Light harvesting enhancement in solar cells with quasicrystalline plasmonic structures. *Opt. Express* **21**, (103), A363–A371 (2013).

[18] Yue, Liyang, Bing Yan, Matthew Attridge, & Zengbo Wang. Light absorption in perovskite solar cell: Fundamentals and plasmonic enhancement of infrared band absorption. *Solar Energy* **124**, 143–152 (2016).

[19] Ferry, V. E. *et al.* Improved red-response in thin film a-Si: H solar cells with soft-imprinted plasmonic back reflectors. *Appl. Phys. Lett.* **95** (18), 183503 (2009).

[20] Pillai, S., Catchpole, K. R., Trupke, T. & Green, M. A.. Surface plasmon enhanced silicon solar cells. *J. Appl. Phys.* **101** (9), 093105 (2007).

[21] Ye, F., Burns, M. J. & Naughton, M. J. Embedded metal nanopatterns for near-field scattering-enhanced optical absorption. *Phys. Status Solidi* **209**, 1829–1834 (2012).

[22] Omelyanovich, M., Ra'di, Y. & Simovski, C. Perfect plasmonic absorbers for photovoltaic applications. *J. Opt.* **17** (12), 125901 (2015).

[23] Elshorbagy, M. H., López-Fraguas, E., Sánchez-Pena, J.M., García-Cámara, B. & Vergaz, R. Boosting ultrathin aSi-H solar cells absorption through a nanoparticle cross-packed metasurface. *Sol. Energy*, **202**, 10–16 (2020).

[24] Liang, C. *et al.* Dual-band infrared perfect absorber based on a Ag-dielectric-Ag multilayer films with nanoring grooves arrays. *Plasmonics*, **15** (1), 93–100 (2020).

[25] Patel, S. K. *et al.* Multi-layered graphene silica-based tunable absorber for infrared wavelength based on circuit theory approach. *Plasmonics* (2020) doi:10.1007/s11468-020-01191-x.

[26] Liang, C. *et al.* A broadband and polarization-independent metamaterial perfect absorber with monolayer Cr and Ti elliptical disks array. *Results Phys.* **15**, 102635 (2019).

[27] Li, H., Niu, J. & Wang, G. Dual-band, polarization-insensitive metamaterial perfect absorber based on monolayer graphene in the mid-infrared range. *Results Phys.* **13**, 102313 (2019).

[28] Zhang, M. & Song, Z. Terahertz bifunctional absorber based on a graphene-spacer-vanadium dioxide-spacer-metal configuration. *Opt. Express*, **28** (8), 11780–11788 (2020).

[29] Varlamov, S., Rao, J. & Soderstrom, T. Polycrystalline silicon thin-film solar cells with plasmonic-enhanced light-trapping. *J. Vis. Exp.* **65**, e4092 (2012).

[30] Morawiec, S., Mendes, M. J., Priolo, F. & Crupi, I. Plasmonic nanostructures for light trapping in thin-film solar cells. *Mater. Sci. Semicond. Process*, **92**, 10–18 (2019).

[31] Thompson, C. V. Solid-state dewetting of thin films. *Ann. Rev. Mater. Res.* **42**, 399–434 (2012).

[32] Pfeiffer, T. V. *et al.* Plasmonic nanoparticle films for solar cell applications fabricated by size-selective aerosol deposition. *Energy Procedia* **60**, 3–12 (2014).

[33] Fernández-Arias M. *et al.* Synthesis and Deposition of Ag Nanoparticles by Combining Laser Ablation and lectrophoretic Deposition Techniques. *Coatings* **9**, 571 (2019).

[34] Novotny, L., & Hecht, B. *Principles of nano-optics.* (Cambridge University Press, New York, USA, 2012).

[35] Johnson, P. B. & Christy, R. W. Optical constants of the noble metals. *Phys. Rev. B*, **6** (12), 4370–4379 (1972).

[36] Weiner, J. & Nunes, F. *Light-matter interaction 2/E.* (Oxford University Press, 2017).